Journal of Superconductivity and Novel Magnetism (2021) 34:1297–1301
https://doi.org/10.1007/s10948-021-05885-z

LETTER

Pinning behavior in bulk MgB_2 prepared using boron powder refined via high-energy ultra-sonication

Sai Srikanth Arvapalli[1] · Muralidhar Miryala[1] · Milos Jirsa[2] · Naomichi Sakai[1] · Masato Murakami[1]

Received: 17 March 2021 / Accepted: 6 April 2021

Abstract
We successfully refined cheap commercial boron powder by means of high-energy ultra-sonication and utilized it in synthesis of bulk MgB_2. Rietveld phase analysis of X-ray diffraction pattern revealed completely formed MgB_2 with a low amount of MgO. MgB_2 bulk prepared of boron ultra-sonicated in ethanol for 15 min showed self-field J_c of around 300 kA/cm^2 at 20 K without any compromise in T_c (~39 K). Pinning analysis based on Dew-Hughes expression showed major pinning contribution from grain-boundary pinning (~95.5%), along with a slight contribution from point pinning (4.5%). The microstructure study detected a system of large MgB_2 grains (hundreds nm large) and 10–20 nm sized particles, possibly Mg-B-O, formed at MgB_2 grain boundaries.

Keywords Flux pinning · Bulk MgB_2 · Boron refinement · Ultrasonication

1 Introduction

Superconductivity in MgB_2 was discovered by Jun Akimitsu et al. in 2001 [1]. Since then, a huge amount of research on the material was done all around the world. Due to uniform trapped field, and cheap and simple processing, MgB_2 is suitable for several superconductor applications such as bulk magnets for compact MRI and NMR, electric motors, etc. [2–4]. Furthermore, its light weight is an important feature that might be crucial for some applications, especially space ones [5]. Although T_c is lower (39 K) compared to cuprates ($YBa_2Cu_3O_{7-\delta}$ ~ 93 K [6], $Bi_2Sr_2Ca_2Cu_3O_{10}$ ~ 105 K [7], etc.), the processing time is shorter and fabrication is easy. These features make the material attractive for mass production and device design. Despite these great advantages, J_c of MgB_2 is only moderate and the compound cannot be cooled into superconducting state by liquid nitrogen. It also exhibits a poor volume density when prepared via conventional sintering. Numerous studies are in progress to address these issues to make MgB_2 commercially attractive. Density can be highly improved via high-pressure techniques such as spark plasma sintering and hot isostatic pressing. While the low T_c prevents use of common and cheap liquid N_2 for MgB_2 cooling, instead of the expensive liquid He, one can use the moderately priced liquid Ne (27 K) or H_2 (23 K). Cryogen-free cooling technique has also been recently developed, reaching just the temperature range of MgB_2 superconductivity [8]. An extensive research was also done to improve J_c of MgB_2 bulk superconductors. The main factor for improving J_c is flux pinning strengthening. In general, defects close to coherence length of the superconducting matter act as flux pinning centers, usually dislocations, lattice defects, etc. Compared to cuprates, MgB_2 has a large coherence length and therefore grain boundaries act as prominent flux pinning centers. In our earlier works, we studied the phase diagrams and optimized sintering time and temperature for obtaining finer MgB_2 grains while avoiding all unreacted precursors [9]. This fine-grained matrix showed improved J_c due to a higher grain boundary density—more flux pinning centers in the matrix. Elsewhere, J_c was improved by adding dopants that either refined the microstructure or acted as flux pinning centers themselves. Variety of dopants was used such as metals, oxides, and carbon sources [10–18]. Of all the dopants, carbon showed the highest increment due to its

✉ Muralidhar Miryala
miryala1@shibaura-it.ac.jp

[1] Graduates School of Science and Engineering, Regional Environment System, Superconducting Material Laboratory, Shibaura Institute of Technology, 3-7-5 Toyosu, Koto-Ku, Tokyo 135-8548, Japan

[2] Institute of Physics ASCR, Na Slovance 2, CZ-18221 Praha 8, Czech Republic

Published online: 08 May 2021

substitution into boron sites. In our recent studies, we used a commercially prepared amorphous nano-boron precursor, which resulted in huge J_c improvement [19]. This study showed that the boron precursor morphology hugely influences the final microstructure of sintered MgB_2 bulk and has a strong dependence on grain boundary pinning. Later, we have used carbon-encapsulated boron precursor, which is an amorphous nano-boron coated with carbon [20]. The MgB_2 bulk produced from this precursor showed huge J_c improvement at self-field as well as at high fields. However, these commercial powders are three times more expensive that the conventional boron. The same effect, without using expensive precursors, was finally achieved by employing high-energy ultra-sonication (HEU). This technique is used to refine the regular conventional boron into nano-sized particles.

In the present work, we discuss the effect of HEU-processed boron on the final microstructure of MgB_2 bulk and its implications on J_c and flux pinning properties. HEU with 50% power was used to refine boron for 15 min that ultimately resulted in 36% J_c improvement. A peculiar microstructure was also observed, which revealed various pinning centers.

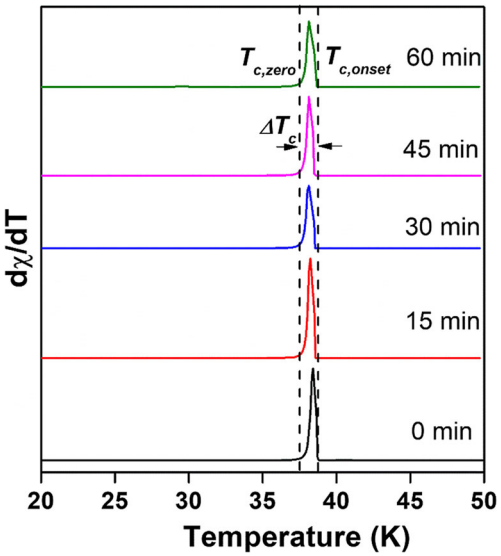

Fig. 2 First-order differential of DC susceptibility vs temperature of various HEU boron-based MgB_2 bulks

2 Fabrication and characterization

Regular conventional boron (Furu-uchi Chemicals, 300 mesh) was ultra-sonicated in ethanol for 15 min and used to fabricate sintered bulk MgB_2. Details of boron ultra-sonication can be found elsewhere [21]. Mg powder and HEU boron powder were mixed in a glove box in argon atmosphere. Later, the mixture was pelletized and sintered in tube furnace (in Ar flow) for 3 h at 775 °C. The processed bulks were characterized with Rigaku SmartLab X-ray powder diffractometer (XRD-RINT2200), Rietveld analysis of the refined phase fraction using diffraction (MAUD) software, field-emission scanning electron microscope (FESEM – JEOL/JSM-7100F), and superconducting quantum interference device (SQUID magnetometer - Quantum Design, model MPMS5). Furthermore, extended Bean critical state model formula was used to estimate J_c and Dew-Hughes expression was used to model the flux pinning diagrams [22].

3 Results and discussion

XRD of HEU boron shows no signs of B_2O_3 phase, which promotes MgO phase that is detrimental to superconductivity of MgB_2 bulk [21]. The average size of boron powder before ultra-sonication is a few microns, while after the ultra-sonication is sub-micron to a few hundred nanometers. Simultaneously, XRD of MgB_2 bulk also shows a very low amount of MgO impurity. Rietveld phase fraction analysis of the bulk showed only 3.6 wt% of MgO, which is less than

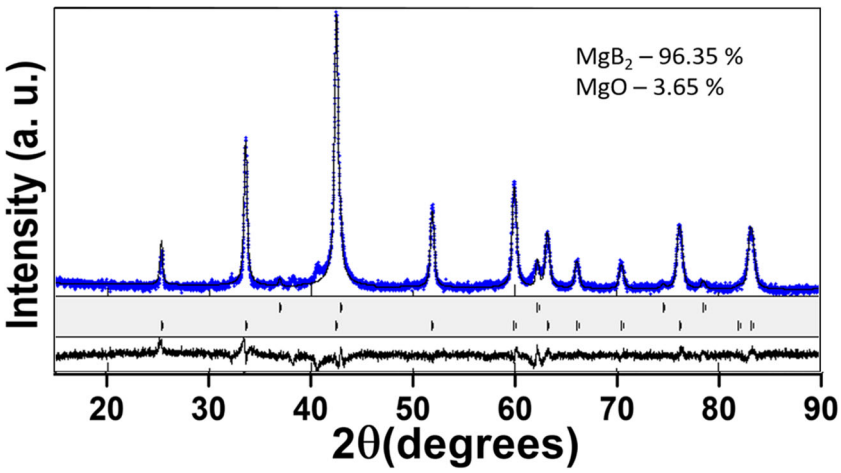

Fig. 1 Rietveld phase fraction analysis of 15 min HEU boron-based MgB_2. A tiny MgO impurity phase was observed

what we observed in conventional MgB_2 before (Fig. 1). The differential susceptibility vs temperature curves show that all the bulks have $T_{c,onset}$ close to 38.5 K and the transition width (calculated from the width of peak of $d\chi/dT$ curves), ΔT_c, is for all the bulks about 0.7 K (Fig. 2) which indicates high quality of the fabricated bulks. The critical current density was calculated using the extended Bean critical state model. Figure 3 shows the superiority of HEU-based bulks' J_c over conventional bulk at various fields. Fifteen minutes of ultra-sonication is best for obtaining high-performance MgB_2 bulk. The self-field J_c value was around 300 kA/cm^2, by 35% more than in a normal bulk—220 kA/cm^2 [21]. Longer ultra-sonication resulted in boron agglomeration that led to large MgB_2 grains reducing J_c. A more detailed explanation can be found elsewhere [21].

Flux pinning diagrams were estimated to determine the pinning mechanism, using Dew-Hughes general expression [23]:

$$f_p = \mathrm{A}(h)^{\mathrm{p}}(1-h)^{\mathrm{q}} \quad (1)$$

where the normalized flux pinning force density is $f_p = F_p / F_{p,max}$ and the reduced magnetic field is $h = H/H_{irr}$. The irreversibility field, H_{irr}, was determined as the field where J_c fell down to 100 A/cm^2, a standard practice in our works. Dew-Hughes suggested that the peak position of $f_p(h)$ dependence indicates the type of pinning in the material. In terms of this model, peak position at 0.2 implies grain boundary pinning, at 0.33 implies δT_c pinning, etc. In the MgB_2 bulks, we observed the peak position located at 0.22 (Fig. 4), slightly above 0.2. In one of our earlier works, where amorphous nano-boron was used, the grain boundary density intentionally increased resulting in a huge boost in self-field J_c. In addition, the $f_p(h)$ peak position was around 0.17, which signified full responsibility of grain boundaries for vortex pinning [19]. On the other hand, when carbon-encapsulated boron was used, the peak position shifted to 0.23, likely due to defects and strain created by carbon substitution [20]. From these two scenarios, it can be postulated that when grain boundaries are sole contributors of flux pinning, the peak position shifts toward lower h values (< 0.2) and when other forms of pinning are active, the peak position shifts to the higher values (> 0.2). This also justifies why grain boundaries are known as low-field pinning centers in MgB_2 superconducting system. In the above context, since the peak position of present MgB_2 bulk prepared from ultra-sonicated boron is above 0.2, we believe that the flux pinning is mostly from grain boundaries but slightly affected by another pinning mechanism.

In the same bulk, we previously tried to fit the experimental curve by Eq. (1) with free pinning parameters (p, q), which led to the values $p \sim 0.7$, $q \sim 2.6$, different from any of the theoretical settings. We also tried to correlate microstructure with pinning mechanisms. FE-SEM images showed two different types of microstructure. One with refined MgB_2 grains with dimensions up to 100 nm, which make up the majority of matrix, and numerous 10–20-nm-sized particles at the pore surfaces (Fig. 5). We consider these tiny nano-particles to be Mg-B-O, which was observed previously in the MgB_2 bulk system [24]. These particles are usually formed when boron dissolves in MgO or reacts with Mg and oxygen, forming a solid solution during sintering at a high sintering temperature. The morphology of the Mg-B-O phase usually varies with temperature. Depending on the sintering temperature, the Mg-B phases are formed as 5–20-nm-thick layers or 5–10-nm particles [25]. These microstructural evidences inspired us to think that these tiny nano Mg-B-O particles might contribute to pinning. We tried to calculate the contribution of point pinning in addition to conventional grain boundary pinning by using the expression suggested by Koblischka et al. [26]:

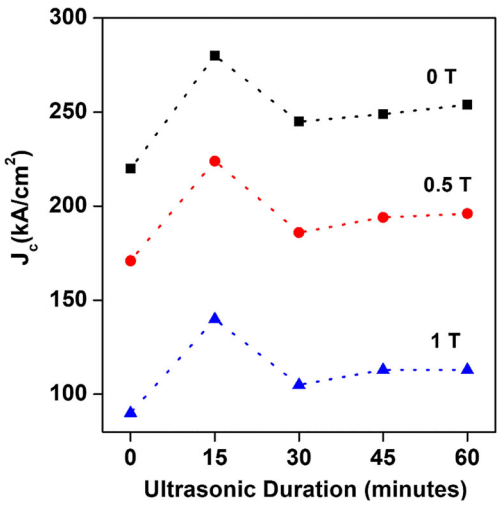

Fig. 3 Critical current density (J_c) of various HEU boron-based MgB_2 bulks at magnetic fields of 0, 0.5, and 1 T, 20 K

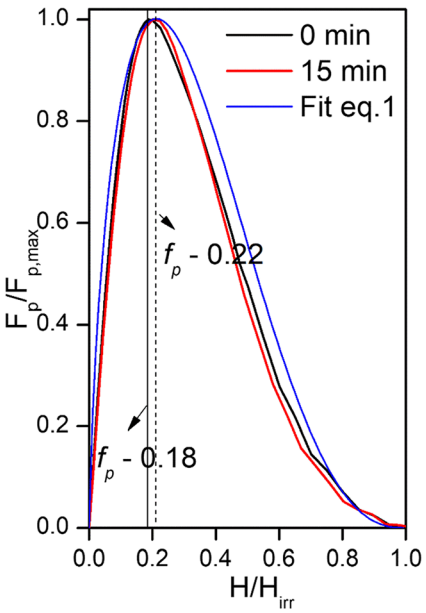

Fig. 4 Flux pinning diagram of 15 min HEU boron-based MgB_2. Peak position slightly shifted right

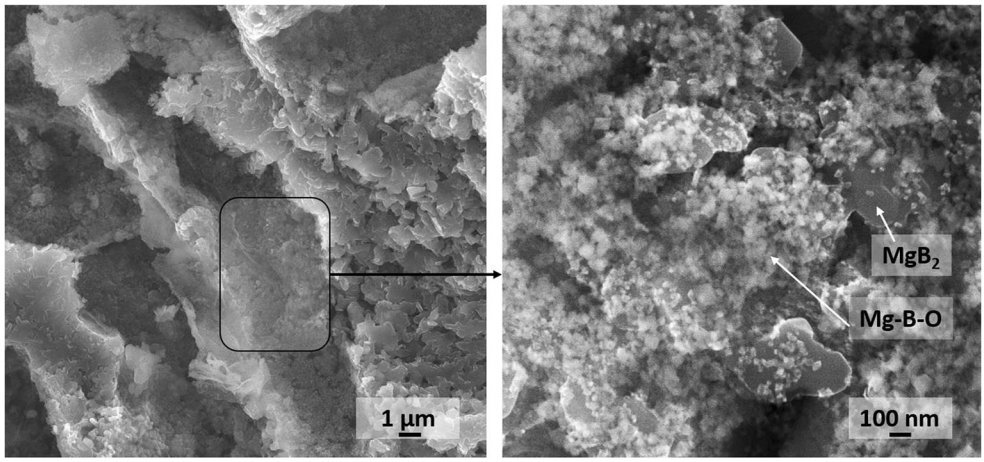

Fig. 5 Pore wall FE-SEM images of 15 min HEU boron-based MgB_2. Tiny Mg-B-O particles can be observed

$$f_p = \mathrm{w}*\left[\mathrm{A}_1(h)^{\mathrm{p}1}(1-h)^{\mathrm{q}1}\right] + (1-\mathrm{w})*\left[\mathrm{A}_2(h)^{\mathrm{p}2}(1-h)^{\mathrm{q}2}\right] \quad (2)$$

$p1 = 0.5$ and $q1 = 2$ (grain boundary pinning), $p2 = 1$ and $q2 = 2$ (point pinning), A_1 and A_2 being constants, and w a weight factor. By fitting the experimental data for 15 min ultra-sonicated MgB_2 with Eq. (2), we arrived at $A_1 \sim 3.6$, $A_2 \sim 3.2$, and $w \sim 0.9545$ that indicated that nearly 95.5 % of pinning came from grain boundaries, with the rest (4.5%) being point pinning. This is probably the reason for the slight shift in the peak position. The contribution from point pinning is very low, due to formation of nano-Mg-B-O particles only on the pore surfaces rather than inside the matrix. The model curve (blue) in Fig. 4 is slightly broader than both experimental curves. The reason is that the theoretical model did not take into account anisotropy and other factors associated with the polycrystalline nature of MgB_2 bulks [27].

4 Conclusion

The high-energy ultra-sonication is a cost-effective way to refine boron, which hugely improves J_c of MgB_2. The superconducting bulk quality is very high, as evidenced by the Rietveld phase fraction analysis of XRD patterns and by the low peak width of the differential susceptibility curves. Bulk matrix consists of MgB_2 particles with dimensions around 500–100 nm. Flux pinning diagrams revealed that the majority of flux pinning is from grain boundaries. Detailed assessment of flux pinning diagrams revealed a little contribution from point pinning as well. Micrographs identified numerous nano-sized Mg-B-O particles on the pore surfaces, which might cause the slight shift of the peak in the flux pinning diagram (Fig. 4) towards values higher than 0.2.

Funding This work was partly supported by the Shibaura Institute of Technology (SIT) Research Center for Green Innovation and Grant-in-Aid FD research budget code: 112282. One of the authors (SSA) received support from SIT for his doctoral program. Milos Jirsa received support from the program Strategy AV 21-VP3 "Energy storage in flywheels."

References

1. Nagamatsu, J., Nakagawa, N., Muranaka, T., Zenitani, Y., Akimitsu, J.: Superconductivity at 39 K in copper doping magnesium diboride. *Nature*. ***410***, 63–64 (**2001**)
2. Vinod, K., Abhilash Kumar, R.G., Syamaprasad, U.: Prospects for MgB_2 superconductors for magnet application. *Supercond. Sci. Technol.* ***20***, R1 (**2007**). https://doi.org/10.1088/0953-2048/20/1/R01
3. Baig, T., Al Amin, A., Deissler, R.J., Sabri, L., Poole, C., Brown, R.W., Tomsic, M., Doll, D., Rindfleisch, M., Peng, X., et al.: Conceptual designs of conduction cooled MgB2 magnets for 1.5 and 3.0 T full body MRI systems. *Supercond. Sci. Technol.* ***30***, 043002 (32pp) (**2017**). https://doi.org/10.1088/1361-6668/aa609b
4. Tomsic, M., Rindfleisch, M., Yue, J., Mcfadden, K., Phillips, J., Sumption, M.D., Bhatia, M., Bohnenstiehl, S., Collings, E.W.: Overview of MgB_2 superconductor applications. *Int. J. Appl. Ceram. Technol.* ***4***, 250–259 (**2007**). https://doi.org/10.1111/j.1744-7402.2007.02138.x
5. Schlachter, S.I., Goldacker, W., Frank, A., Ringsdorf, B., Orschulko, H.: Properties of MgB_2 superconductors with regard

to space applications. *Cryogenics (Guildf).* ***46***, 201–207 (**2006**). https://doi.org/10.1016/j.cryogenics.2005.11.003
6. Wu, M.K., Ashburn, J.R., Torng, C.J., Hor, P.H., Meng, R.L., Gao, L., Huang, Z.J., Wang, Y.Q., Chu, C.W.: Superconductivity at 93 K in a new mixed-phase Yb-Ba-Cu-O compound system at ambient pressure. *Phys. Rev. Lett.* ***58***, 908–910 (**1987**). https://doi.org/10.1103/PhysRevLett.58.908
7. Maeda, H., Tanaka, Y., Fukutomi, M., Asano, T.: A New High- Tc Oxide Superconductor without a Rare Earth Element. *Jpn. J. Appl. Phys.* ***27***, L209–L210 (**1988**). https://doi.org/10.1143/JJAP.27.L209
8. Morandi, A., Fiorillo, A., Pullano, S., Ribani, P.L.: Development of a Small Cryogen-Free MgB2 Test Coil for SMES Application. *IEEE Trans. Appl. Supercond.* ***27***, 1–4 (**2017**). https://doi.org/10.1109/TASC.2017.2653202
9. Muralidhar, M., Inoue, K., Koblischka, M.R., Tomita, M., Murakami, M.: Optimization of processing conditions towards high trapped fields in MgB_2 bulks. *J. Alloys Compd.* ***608***, 102–109 (**2014**). https://doi.org/10.1016/j.jallcom.2014.04.017
10. Kirat, G., Kizilaslan, O., Aksan, M.A., Yakinci, M.E.: Effect of Co addition on the critical current density of MgB2 superconductor. *Phys. B Condens. Matter.* ***445***, 24–27 (**2014**). https://doi.org/10.1016/j.physb.2014.03.072
11. Pan, X.F., Shen, T.M., Li, G., Cheng, C.H., Zhao, Y.: Doping effect of Pr6O11 on superconductivity and flux pinning of MgB2 bulk. *Phys. Status Solidi.* ***204***, 1555–1560 (**2007**). https://doi.org/10.1002/pssa.200622505
12. Zhu, Y., Matsumoto, A., Senkowicz, B.J., Kumakura, H., Kitaguchi, H., Jewell, M.C., Hellstrom, E.E., Larbalestier, D.C., Voyles, P.M.: Microstructures of SiC nanoparticle-doped MgB2 Fe tapes. *J. Appl. Phys.* ***102***, 013913 (**2007**). https://doi.org/10.1063/1.2750409
13. Kim, J.H., Zhou, S., Hossain, M.S.A., Pan, A.V., Dou, S.X.: Carbohydrate doping to enhance electromagnetic properties of MgB 2 superconductors. *Appl. Phys. Lett.* ***89***, 3–6 (**2006**). https://doi.org/10.1063/1.2358947
14. Gao, Z., Ma, Y., Zhang, X., Wang, D., Yu, Z., Yang, H., Wen, H., Mossang, E.: Enhancement of the critical current density and the irreversibility field in maleic anhydride doped Mg B2 based tapes. *J. Appl. Phys.* **102**, *102* (**2007**). https://doi.org/10.1063/1.2748711
15. Matsumoto, A., Kumakura, H., Kitaguchi, H., Hatakeyama, H.: Effect of SiO2 and SiC doping on the powder-in-tube processed MgB2 tapes. *Supercond. Sci. Technol.* ***16***, 926–930 (**2003**). https://doi.org/10.1088/0953-2048/16/8/317
16. Pan, X.F., Cheng, C.H., Zhao, Y.: Effect of rare-earth oxides doping on the superconductivity and flux pinning of MgB_2 superconductor. *J. Supercond. Nov. Magn.* ***24***, 1611–1616 (**2011**). https://doi.org/10.1007/s10948-010-1066-4
17. Peng, J., Liu, Y., Ma, Z., Shahriar Al Hossain, M., Xin, Y., Jin, J.: Superior critical current density obtained in MgB2bulks via employing carbon-coated boron and minor Cu addition. *Phys. C Supercond. Appl.* ***528***, 60–64 (**2016**). https://doi.org/10.1016/j.physc.2016.07.016
18. Muralidhar, M., Higuchi, M., Jirsa, M., Diko, P., Kokal, I., Murakami, M.: Improved Critical Current Densities of Bulk MgB_2 Using Carbon-Coated Amorphous Boron. *IEEE Trans. Appl. Supercond.* ***27***, 18–21 (**2017**)
19. Arvapalli, S.S., Muralidhar, M., Murakami, M.: High-Performance Bulk MgB2 Superconductor Using Amorphous Nano-boron. *J. Supercond. Nov. Magn.* ***32***, 1891–1895 (**2018**)
20. Arvapalli, S.S., Miryala, M., Murakami, M.: Beneficial Impact of Excess Mg on Flux Pinning in Bulk MgB2 Synthesized with Ag Addition and Carbon Encapsulated Boron. *Adv. Eng. Mater.* ***21***, (7pp), 1900497 (**2019**). https://doi.org/10.1002/adem.201900497
21. Arvapalli, S.S., Miryala, M., Jirsa, M., Murakami, M., Sai Srikanth, A., Muralidhar, M., Milos, J., Murakami, M.: Size reduction of boron particles by high-power ultrasound for optimization of bulk MgB_2. *Supercond. Sci. Technol.* ***33***, 115009 (**2020**). https://doi.org/10.1088/1361-6668/abb63e
22. Bean, C.P.: Magnetization of high-field superconductors. *Rev. Mod. Phys.* ***36***, 31–39 (**1964**). https://doi.org/10.1103/RevModPhys.36.31
23. Dew-Hughes, D.: Flux pinning mechanisms in type II superconductors. *Philos. Mag.* ***30***, 293–305 (**1974**). https://doi.org/10.1080/14786439808206556
24. You, A., Be, M.A.Y., In, I.: $Mg(B,O)_2$ precipitation in MgB_2. *J. Appl. Phys.* ***93***, 6208 (**2003**). https://doi.org/10.1063/1.1568528
25. Prikhna, T.A., Eisterer, M., Weber, H.W., Gawalek, W., Kovylaev, V.V., Karpets, M.V., Basyuk, T.V., Moshchil, V.E.: Nanostructural inhomogeneities acting as pinning centers in bulk MgB_2 with low and enhanced grain connectivity. *Supercond. Sci. Technol.* ***27***, 044013 (9pp) (**2014**). https://doi.org/10.1088/0953-2048/27/4/044013
26. Koblischka, M.R., Muralidhar, M.: Pinning force scaling analysis of Fe-based high-T_c superconductors. *Int. J. Mod. Phys. B.* ***30***, 1630017 (**2016**). https://doi.org/10.1142/S0217979216300176
27. Jirsa, M., Rames, M., Koblischka, M.R., Koblischka-Veneva, A., Berger, K., Douine, B.: Relaxation and pinning in spark-plasma sintered MgB_2 superconductor. *Supercond. Sci. Technol.* ***29***, 025006 (7pp) (**2016**). https://doi.org/10.1088/0953-2048/29/2/025006